

## Rapid Communications

The Rapid Communications section is intended for the accelerated publication of important new results. Since manuscripts submitted to this section are given priority treatment both in the editorial office and in production, authors should explain in their submittal letter why the work justifies this special handling. A Rapid Communication in Physical Review D should be no longer than five printed pages and must be accompanied by an abstract. Page proofs are sent to authors, but because of the accelerated schedule, publication is not delayed for receipt of corrections unless requested by the author or noted by the editor.

### New measurement of the production polarization and magnetic moment of the $\Xi^-$ hyperon

L. H. Trost, E. R. McCliment, and C. R. Newsom

Department of Physics and Astronomy, University of Iowa, Iowa City, Iowa 52242

S. Y. Hsueh,<sup>(a)</sup> D. Müller, J. Tang, R. Winston, and G. Zapalac<sup>(b)</sup>  
 Enrico Fermi Institute, The University of Chicago, Chicago, Illinois 60637

E. C. Swallow

Department of Physics, Elmhurst College, Elmhurst, Illinois 60126  
 and Enrico Fermi Institute, The University of Chicago, Chicago, Illinois 60637

J. P. Berge, A. E. Brenner,<sup>(c)</sup> P. S. Cooper, P. Grafström,<sup>(d)</sup> E. Jastrzembki,<sup>(e)</sup> J. Lach,  
 J. Marriner, R. Raja, and V. J. Smith<sup>(f)</sup>  
 Fermi National Accelerator Laboratory, Batavia, Illinois 60510

E. W. Anderson

Department of Physics, Iowa State University, Ames, Iowa 50011

A. S. Denisov, V. T. Grachev, V. A. Schegelsky, D. M. Seliverstov, N. N. Smirnov, N. K. Terentyev,  
 I. I. Tkatch, and A. A. Vorobyov  
 Leningrad Nuclear Physics Institute, Leningrad, U.S.S.R.

P. Razis<sup>(g)</sup> and L. J. Teig<sup>(h)</sup>

J. W. Gibbs Laboratory, Yale University, New Haven, Connecticut 06511

(Received 8 May 1989)

We have measured the production polarization and magnetic moment of a sample of  $89 \times 10^3 \Xi^-$  hyperons produced in the inclusive reaction  $p(400 \text{ GeV}/c) + \text{Cu} \rightarrow \Xi^- + X$ . The weighted average of the polarization is  $-0.070 \pm 0.008 \pm 0.010$  at a  $p_t$  of  $0.63 \text{ GeV}/c$ . The  $\Xi^-$ 's magnetic moment yields the value  $\mu_{\Xi} = -0.661 \pm 0.036 \pm 0.036$  nuclear magnetons. The first error is statistical, the second systematic.

The experimental values of baryon magnetic moments provide a sensitive means to test the various quark models of elementary particles. Previous measurement of the  $\Xi^-$ 's magnetic moment by Rameika *et al.* disagreed with the predictions of the naive quark model, prompting many refinements of the model.<sup>1,2</sup> In this work we present new measurements of the  $\Xi^-$  production polarization and magnetic moment from data collected in experiment E715 at Fermilab.<sup>3</sup>

In this experiment a secondary beam containing a 0.5% admixture of  $\Xi^-$  with an average momentum of approximately  $250 \text{ GeV}/c$  was inclusively produced by collisions of  $400\text{-GeV}/c$  protons on a copper target. The  $\Xi^-$  polarization was determined from a set of events containing the decay chain  $\Xi^- \rightarrow \Lambda^0 + \pi^-$  followed by  $\Lambda^0 \rightarrow p + \pi^-$ .

These events were selected from a sample containing only charged particles in the final state.

Parity conservation requires the  $\Xi^-$  polarization to be normal to the production plane (parallel or antiparallel to the vector product  $\mathbf{p}_{\text{inc}} \times \mathbf{p}_{\Xi}$ , where  $\mathbf{p}_{\text{inc}}$  is the momentum of the incident proton and  $\mathbf{p}_{\Xi}$  the momentum of the  $\Xi^-$ ). By convention, positive polarization is in the direction of positive cross product. The targeting angle  $\theta_t$  between the incident proton and the  $\Xi^-$  can be varied by means of dipole magnets upstream of the target. Data were taken with the production plane both horizontal (horizontal targeting) and vertical (vertical targeting).<sup>4</sup> In each production mode two different targeting angles were selected. For vertical targeting these angles were  $+3.07$  and  $-2.01$  mrad with an average secondary beam momentum of

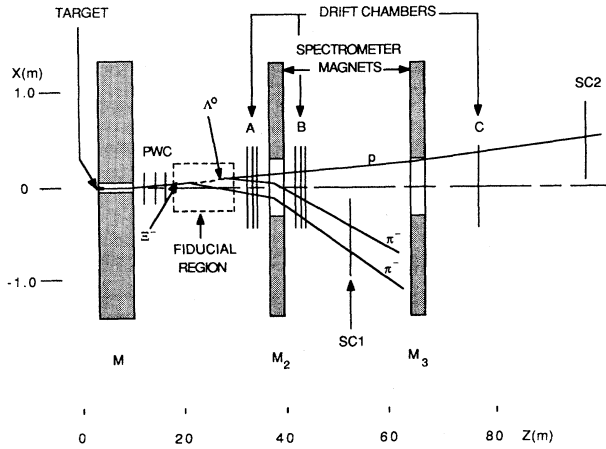


FIG. 1. Experimental apparatus.

244.7 GeV/c. For horizontal targeting the angles were +2.10 mrad with momentum 237.5 GeV/c and -3.06 mrad with momentum 253.5 GeV/c.

The E715 apparatus is described in detail in Ref. 3. The parts relevant to this experiment along with a superimposed  $\Xi^-$  decay chain are shown schematically in Fig. 1. They include the following: the three magnets  $M_1$ ,  $M_2$ , and  $M_3$ ; the system of proportional wire chambers (PWC's); drift-chamber clusters  $A$ ,  $B$ , and  $C$ ; and the various scintillators used in the trigger. Magnet  $M_1$  has a length of 7.3 m and a field integral of 17.6 Tm, giving a bend angle of 21 mrad at a momentum of 250 GeV/c. The PWC's are used in conjunction with this magnet to measure the momentum of the  $\Xi^-$  prior to its decay. The calibration and resolution of the PWC system is discussed in detail in Ref. 3. Overall the momentum resolution of the secondary beam is  $\Delta p/p = \pm 0.7\%$  ( $1\sigma$ ).

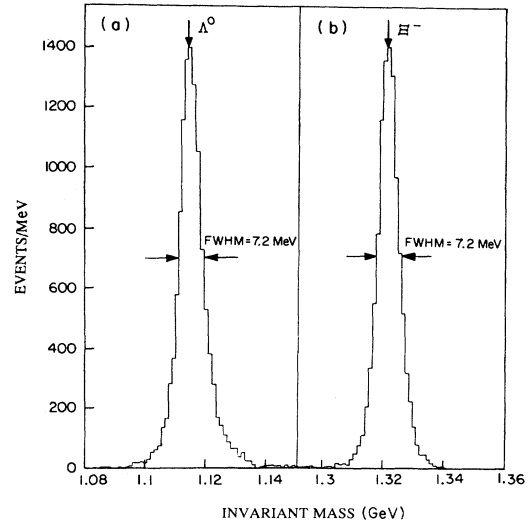


FIG. 2. Invariant-mass spectra. (a) Uses hypothesis that positive and negative downstream tracks are proton and  $\pi^-$ , respectively. Peak is centered on  $\Lambda^0$  mass indicated by the vertical arrow. (b) Uses hypothesis that the decay products of beam particles are  $\Lambda^0$  and  $\pi^-$ . Peak is centered on  $\Xi^-$  mass.

The momenta of the decay products are measured by a downstream spectrometer consisting of magnets  $M_2$  and  $M_3$  and drift-chamber clusters  $A$ ,  $B$ , and  $C$ . Clusters  $A$  and  $B$  and magnet  $M_2$  determine the momentum of the pions and, in conjunction with magnet  $M_3$  and cluster  $C$ , the proton momentum. Overall, the downstream spectrometer has the following resolution for both pions and protons:  $\Delta(1/p) = 0.0004$  (GeV/c) $^{-1}$ ,  $\Delta\theta = 150 \mu\text{rad}$  (azimuth), and  $\Delta\phi = 50 \mu\text{rad}$  (dip). The momentum distributions measured by the downstream spectrometer are in agreement with Monte Carlo studies using our three-

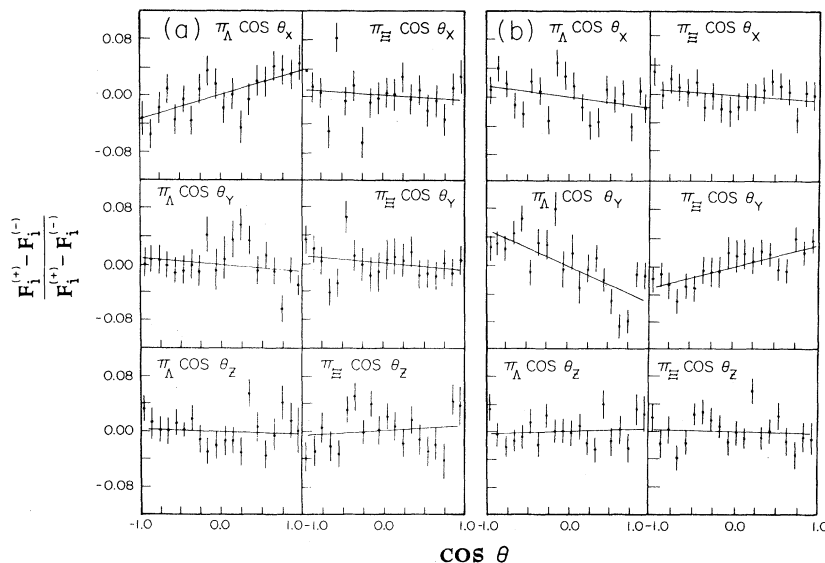


FIG. 3. Experimental angular distributions of decay pions. (a) Vertical targeting. (b) Horizontal targeting. The solid lines represent a one-parameter least-squares fit to the experimental points.

TABLE I.  $\Xi$  Polarization components. The numbers in parentheses are the  $\chi^2$ /(number of degrees of freedom). The errors are statistical.

	$x$	$y$	$z$
	Horizontal targeting		
From $\pi_\Lambda$	$0.008 \pm 0.017$ (0.85)	$0.104 \pm 0.017$ (1.24)	$-0.031 \pm 0.018$ (1.06)
From $\pi_\Xi$	$-0.014 \pm 0.021$ (1.23)	$0.064 \pm 0.019$ (0.94)	$-0.009 \pm 0.022$ (1.03)
Best fit	$0.002 \pm 0.013$ (0.66)	$0.082 \pm 0.012$ (0.52)	$-0.022 \pm 0.014$ (1.08)
	Vertical targeting		
From $\pi_\Lambda$	$-0.079 \pm 0.15$ (0.81)	$0.006 \pm 0.014$ (1.08)	$0.008 \pm 0.016$ (0.91)
From $\pi_\Xi$	$-0.024 \pm 0.018$ (1.38)	$-0.011 \pm 0.017$ (0.90)	$0.026 \pm 0.019$ (1.01)
Best fit	$-0.057 \pm 0.011$ (1.23)	$-0.001 \pm 0.011$ (0.93)	$0.016 \pm 0.012$ (0.85)

prong  $\Xi$ -decay hypothesis.

The entire system is aligned using beam tracks with the magnets off. The magnets  $M_2$  and  $M_3$  have been calibrated previously; they impart a known transverse momentum  $p_t$ , which is approximately 0.8 GeV/c. As a check on the consistency of the calibration we demand overall momentum conservation in the mean, and the invariant-mass distributions (Fig. 2) that we use for event selection must be centered on the accepted masses of the  $\Lambda^0$  and  $\Xi^-$ .<sup>5</sup>

The trigger for cascade decays with three charged tracks in the final state consists of an upstream beam trigger, a negative-track scintillator SC1, a positive-track scintillator SC2, and a downstream beam veto. The raw data sample satisfying the trigger requirement contained approximately  $4 \times 10^6$  events. The final  $\Xi^-$  decay sample was obtained as follows: First events were selected that have a beam track and at least two negative tracks and one positive track downstream. The reconstruction of a  $\Lambda^0$  using two downstream tracks, one positive and one negative, were then required of these events. Next the reconstruction of a  $\Xi^-$  from a second downstream negative track not associated with the  $\Lambda^0$  and the upstream beam track was required. At this stage only loose cuts of  $\pm 30$  MeV on either mass were imposed. The invariant-mass distributions in Fig. 2 are centered on the expected values (see Ref. 5) and fall within the specified cuts. The final set of events were then required to pass the following cuts: (1) The  $\Xi^-$  and  $\Lambda^0$  decay vertices must occur within a 14-m fiducial region located between the last chamber of PWC and the first drift chamber of cluster A; (2) the  $\Lambda^0$  decay vertex must be downstream of the  $\Xi^-$  decay vertex by at least  $1\sigma$  (1 m); (3) an opening-angle cut of  $50 \mu\text{rad}$  was imposed on the downstream tracks to conform to the two-particle resolution of the drift chambers; and (4) the cuts on the invariant masses were tightened to  $\pm 20$  MeV.

Ambiguities were resolved as follows. If the event contained more than the requisite two negative tracks (15% of events) the best fit to the mass of the corresponding hyperon was used. If the same pion fit both the  $\Xi$  and  $\Lambda$  hypotheses, we used the vertex to distinguish them provided the vertices were separated by more than  $1\sigma$  ( $\pm 1.0$  m). Events were dropped if we could not resolve the ambiguity ( $< 0.2\%$  of the events). Monte Carlo studies using this procedure reproduce the input polarization within the statistical error ( $1\sigma$ ). The final vertical-targeting data

sample, after all the cuts, contained  $22 \times 10^3$  events at each targeting angle. The horizontal-targeting sample contained  $25 \times 10^3$  events at  $+2.1$  mrad and  $20 \times 10^3$  events at  $-3.1$  mrad.

In the center-of-momentum system (COM) of the  $\Xi^-$  the angular distribution of the pion daughter is given by

$$\frac{dW^{(\pm)}}{d(\cos\theta_i)} = A_i(\cos\theta_i)(1 \mp \alpha_\Xi P_{\Xi i} \cos\theta_i), \quad (1)$$

where  $i = x, y, \text{ or } z$ ,  $\cos\theta_i$  are the components of a unit vector in the pion's momentum direction,  $A_i(\cos\theta_i)$  are the acceptance functions of the apparatus, and  $\alpha_\Xi$  is the asymmetry parameter of the  $\Xi^-$ . The upper (lower) sign is for a positive (negative) targeting angle (reversing the targeting angle reverses the direction of the polarization). A similar relation holds for the  $\Lambda^0$  decay pion in the  $\Lambda^0$  COM with the following replacement:<sup>6</sup>

$$\alpha_\Lambda \rightarrow \alpha_\Xi^{\text{eff}} = \alpha_\Lambda(1 + 2\gamma_\Xi - \alpha_\Xi^2)/3, \quad (2)$$

where  $\gamma_\Xi$  in this expression is another of the  $\Xi^-$ 's asymmetry parameters (see Ref. 5). This means we can obtain a separate measurement of the  $\Xi$  polarization from each decay mode, which provides us with the possibility of checking the consistency and systematic error of our measurements. To extract the polarization we exploit the sign reversal in Eq. (1). We form the difference over the sum of two angular distributions, each having the form of Eq. (3), but one with positive targeting angle, the other nega-

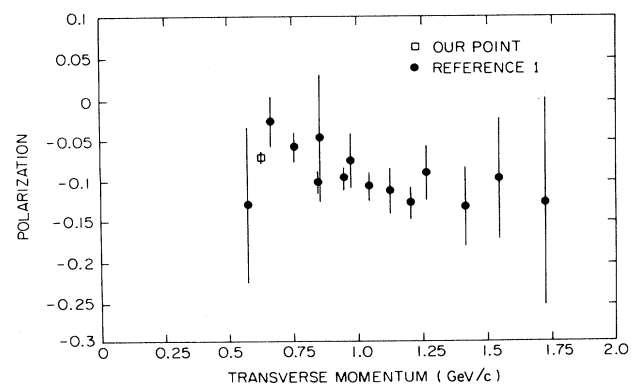


FIG. 4.  $\Xi$  polarization vs transverse momentum.

TABLE II. Summary of the precession angle and the magnetic-moment measurements from vertical-targeting data.

	$\xi$ (rad)	$g/2-1$	$\mu_{\Xi}$ ( $\mu_N$ )
From $\pi_{\Lambda}$	$-0.101 \pm 0.20$	$-0.025 \pm 0.051$	$-0.692 \pm 0.036$ (0.85)
From $\pi_{\Xi}$	$-0.825 \pm 0.52$	$-0.206 \pm 0.135$	$-0.564 \pm 0.094$ (0.96)
Best fit	$-0.274 \pm 0.20$	$-0.069 \pm 0.052$	$-0.661 \pm 0.037$ (0.92)
Ref. 1			$-0.69 \pm 0.04$

tive. Then the acceptance function cancels, giving the result<sup>7</sup>

$$\frac{dW^{(+)} / d(\cos\theta_i) - dW^{(-)} / d(\cos\theta_i)}{dW^{(+)} / d(\cos\theta_i) + dW^{(-)} / d(\cos\theta_i)} = -\alpha_{\Xi} P_{\Xi i} \cos\theta_i. \quad (3)$$

Figure 3 shows the angular distributions for both vertical- and horizontal-targeting data obtained from this equation. The experimental points are determined from the individual  $\cos\theta$  distributions in accordance with the left-hand side of Eq. (3). The  $F_i^{(\pm)}$  are the fractional numbers of events in each bin of the individual  $\cos\theta$  distributions for positive (negative) targeting angles. The solid lines are one-parameter fits to the right-hand side of this equation.<sup>8</sup> The slope of each straight line in Fig. 3 is the corresponding product  $\alpha_{\Xi} P_{\Xi i}$ . The values of  $\alpha_{\Xi}$  and other asymmetry parameters used in the calculation of  $\alpha_{\Xi}^{fit}$  are taken from Ref. 5:  $\alpha_{\Xi} = -0.455 \pm 0.015$ ,  $\gamma_{\Xi} = 0.89 \pm 0.008$ , and  $\alpha_{\Lambda} = 0.642 \pm 0.013$ . With these values taken from the literature the slopes determine the polarization. The polarization components obtained in this manner are listed in Table I along with the reduced  $\chi^2$ 's for the fits. The final results are found in the rows marked "best fit." These values are obtained by fitting the angular distributions of both decay pions simultaneously.

The  $\Xi^-$  polarization is produced perpendicular to the production plane, and the field of magnet  $M_1$  is vertically downward ( $-y$  direction). With horizontal targeting the initial polarization is parallel to the magnetic field and there is no precession, whereas with vertical targeting the polarization is produced along the  $x$  axis and precesses about the  $y$  axis. Upon emerging from the magnet the  $x$  and  $z$  components of polarization must, therefore, be zero for horizontal targeting, and the  $y$  component must be zero for vertical targeting. However, it will be noted that there is a  $2\sigma$  discrepancy between the values of the  $x$  component of polarization in the vertical-targeting case. We have studied this discrepancy, and, to the best of our knowledge, it is a statistical fluctuation. The best values of the polarization components in Table I obtained by an overall fit to both  $\Xi$  and  $\Lambda$  decay are consistent with these requirements. This is supported by the opposite signs of  $P_x$  and  $P_y$  obtained from vertical and horizontal targeting, respectively (see Ref. 4). Our best value of the  $\Xi$  polarization, obtained from a weighted average of the horizontal- and vertical-targeting data is  $P_{\Xi} = -0.070 \pm 0.008 \pm 0.010$ . This value is plotted in Fig. 4 along with values taken from Ref. 1 for comparison.

The magnetic moment is determined from the precession of the polarization. For vertical targeting the angle of precession  $\xi$  is  $\arctan(P_z/P_x)$ . The  $g$  factor is related to the precession angle (in degrees) as follows:

$$\xi = -(13.0 \text{ deg/Tm})(g/2-1) \int B dl, \quad (4)$$

and the magnetic moment is

$$\mu_{\Xi} = -g\mu_N m_p / (2m_{\Xi}), \quad (5)$$

where  $\mu_N$  is the nuclear magneton. The  $\int B dl$  of magnet  $M_1$  in Eq. (3) is inferred from the bend angle and the calibration procedure. It has the value 17.32 Tm. Using this value and combining Eqs. (3) and (4) yields the results for the cascade magnetic moment listed in Table II. This table gives the values obtained from the  $\Xi^-$  and  $\Lambda^0$  decay pions separately and a best value obtained from a simultaneous fit to both decays. Using the best value and including systematic error (discussed below) our result for the magnetic moment is  $\mu_{\Xi} = -0.661 \pm 0.036 \pm 0.036$ . The first error is statistical, the second systematic. This result is consistent with the result  $-0.69 \pm 0.04$ , quoted in Ref. 1. Moreover, our field integral is significantly different from theirs. The combined results are thus free of multiple  $360^\circ$  ambiguities (multiple  $180^\circ$  ambiguities are resolved by the horizontal-targeting results).

The systematic error was determined by studying the change in the results affected by varying the  $\Lambda^0$  and  $\Xi^-$  mass cuts, the fiducial volume cut, and the opening angle cut. In addition the beam momentum distribution was divided into six subsamples with roughly equal numbers of events and the polarization components determined for each subsample. In no case did any measured component of the  $\Xi$  production polarization vary by more than the statistical error at the  $1\sigma$  level. The systematic error for the magnetic moment was deduced from that of the polarizations.

We are grateful to the Fermilab staff, particularly the Proton, Physics, and Computing Departments, for their assistance. This work was supported in part by the U.S. Department of Energy under Contracts No. DE-AC02-87ER40318, No. DE-AC02-80ER10587, No. DE-AC02-76C H03000, and No. DE-AC02-76ER03075, and by the USSR Academy of Sciences. The work of L.H.T. was submitted in partial fulfillment of the requirements of the M.S. degree at the University of Iowa.

- (a) Present address: Fermilab.  
 (b) Present address: Stanford Linear Accelerator Center, Stanford, CA 94305.  
 (c) Present address: Supercomputer Research Center, Institute for Defense Analyses, 4380 Forbes Blvd., Lanham, MD 20706.  
 (d) Present address: EP Division, CERN, CH-1211 Geneva 23, Switzerland.  
 (e) Present address: Brookhaven National Laboratory, Upton, NY 11973.  
 (f) Permanent address: H.H. Wills Physical Laboratory, University of Bristol, Bristol BS8 1TL, England.  
 (g) Present address: Eidgenössische Technische Hochschule, Zurich, Switzerland.  
 (h) Present address: Mitre Corporation, Bedford, MA 01730.
- <sup>1</sup>R. Rameika *et al.*, Phys. Rev. Lett. **52**, 581 (1984).  
<sup>2</sup>A. De Rújula, H. Georgi, and S. L. Glashow, Phys. Rev. D **12**, 147 (1975). For a review of theoretical work through 1983, see A. J. G. Hey and R. L. Kelly, Phys. Rep. **96**, 73 (1983).  
<sup>3</sup>S. Y. Hsueh *et al.*, Phys. Rev. D **38**, 2056 (1988). A complete description of the apparatus, its calibration, and resolution is found in this paper.  
<sup>4</sup>The coordinate system is right handed with  $z$  along the direction of the  $\Xi$  momentum and  $x$  horizontal, putting  $y$  in the vertical plane. With a positive horizontal-targeting angle

$\mathbf{p}_{\text{inc}} \times \mathbf{p}_{\Xi}$  is along the negative  $y$  axis, whereas a positive vertical-targeting angle puts this vector along the positive  $x$  axis. Thus, in the absence of precession, a positive  $x$  component of polarization from vertical targeting corresponds to a negative  $y$  component from horizontal targeting. For each event the coordinate axes rotates in the magnet so that the  $z$  axis remains parallel to the cascade momentum, while the  $x$  axis remains horizontal. The precession of the polarization is thus measured relative to the momentum.

- <sup>5</sup>Particle Data Group, G. P. Yost *et al.*, Phys. Lett. B **204**, 1 (1988).  
<sup>6</sup>S. Gasiorowicz, *Elementary Particle Physics* (Wiley, New York, 1966).  
<sup>7</sup>In our case the targeting angles are not equal and opposite. However, the acceptance still cancels, and one obtains the average of the polarizations at the two targeting angles plus a small nonlinear term that is proportional to the difference of the polarizations. Our results are not sensitive enough to detect the nonlinearity.  
<sup>8</sup>Before doing the one-parameter fit, a two-parameter fit was done with the  $\cos\theta$  distributions folded in half. After ascertaining that the intercept at  $\cos\theta=0$  was consistent with 0, the one-parameter fit was done. Both fits give  $\chi^2/(\text{number of degrees of freedom}) \approx 1$ .